Applied Energy 146 (2015) 298–312

Contents lists available at ScienceDirect

Applied Energy

journal homepage: www.elsevier.com/locate/apenergy

Coal gasification integration with solid oxide fuel cell and chemical looping combustion for high-efficiency power generation with inherent CO_2 capture

Shiyi Chen [a], Noam Lior [b,*], Wenguo Xiang [a]

[a] Key Laboratory of Energy Thermal Conversion and Control of Ministry of Education, School of Energy and Environment, Southeast University, Nanjing 210096, China
[b] Department of Mechanical Engineering and Applied Mechanics, University of Pennsylvania, Philadelphia, PA 19104-6315, USA

HIGHLIGHTS

- A novel power system integrating coal gasification with SOFC and chemical looping combustion.
- The plant net power efficiency reaches 49.8% with complete CO_2 separation.
- Energy and exergy analysis of the entire plant is conducted.
- Sensitivity analysis shows a nearly constant power output when SOFC temperature and pressure vary.
- NiO oxygen carrier shows higher plant efficiency than using Fe_2O_3 and CuO.

ARTICLE INFO

Article history:
Received 14 August 2014
Received in revised form 13 January 2015
Accepted 26 January 2015

Keywords:
Coal gasification
Solid oxide fuel cells
Chemical looping combustion
IGCC
Combined power cycles
CO_2 capture

ABSTRACT

Since solid oxide fuel cells (SOFC) produce electricity with high energy conversion efficiency, and chemical looping combustion (CLC) is a process for fuel conversion with inherent CO_2 separation, a novel combined cycle integrating coal gasification, solid oxide fuel cell, and chemical looping combustion was configured and analyzed. A thermodynamic analysis based on energy and exergy was performed to investigate the performance of the integrated system and its sensitivity to major operating parameters. The major findings include that (1) the plant net power efficiency reaches 49.8% with ~100% CO_2 capture for SOFC at 900 °C, 15 bar, fuel utilization factor = 0.85, fuel reactor temperature = 900 °C and air reactor temperature = 950 °C, using NiO as the oxygen carrier in the CLC unit. (2) In this parameter neighborhood the fuel utilization factor, the SOFC temperature and SOFC pressure have small effects on the plant net power efficiency because changes in pressure and temperature that increase the power generation by the SOFC tend to decrease the power generation by the gas turbine and steam cycle, and v.v.; an advantage of this system characteristic is that it maintains a nearly constant power output even when the temperature and pressure vary. (3) The largest exergy loss is in the gasification process, followed by those in the CO_2 compression and the SOFC. (4) Compared with the CLC Fe_2O_3 and CuO oxygen carriers, NiO results in higher plant net power efficiency. To the authors' knowledge, this is the first analysis synergistically combining in a hybrid system: (1) coal gasification, (2) SOFC, and (3) CLC, which results in a system of high energy efficiency with full CO_2 capture, and advances the progress towards the world's critically needed approach to "clean coal".

1. Introduction

Power plants based on coal feeding produce approximate 50% of the electricity in the United States, and much more, about 70%, in some other countries, such as China and India [1–5]. Among all fuels, coal produces the highest quantity of CO_2 per unit generated heat and electricity, so concerns about global warming have led to much work on effective CO_2 capture and storage (CCS) from power plants. While many methods were proposed for CO_2 capture in the power generation sector, they typically are energy intensive, thus resulting in significantly lowering the plant energy efficiency and in increasing the cost of electricity.

To take advantage of the high efficiency of combined cycles for power generation, which approaches 60%, but most conveniently

* Corresponding author. Tel.: +1 215 898 4803; fax: +1 215 573 6334.
E-mail address: lior@seas.upenn.edu (N. Lior).

http://dx.doi.org/10.1016/j.apenergy.2015.01.100
0306-2619/

Nomenclature

E_D	exergy destruction in the system (kW)
E_F	fuel input exergy into the system (kW)
E_{input}	component exergy input (kW)
E_{output}	component exergy output (kW)
E_P	exergy obtained in the system (kW)
$\dot{E}_s$	exergy of a stream (kW)
$\dot{E}_{s,d}$	exergy destruction rate (kW)
$\dot{E}_{s,i}$	inlet or input exergy (kW)
$\dot{E}_{s,o}$	outlet or product exergy (kW)
$\dot{e}_{ch}$	molar chemical exergy (kJ/mol)
$e_{ch,i}$	standard molar chemical exergy (kJ/mol)
$\dot{e}_{ph}$	molar physical exergy (kJ/mol)
e_{fuel}	fuel exergy (kJ/kg)
$\dot{e}_s$	exergy of a system (kJ/mol)
F	Faraday constant (96486 C/mol)
ΔH	enthalpy of reaction (kJ/mol)
h	enthalpy (kJ/mol)
h_0	enthalpy at the reference state (kJ/mol)
I	current (A)
LHV_{coal}	coal lower heating value (kJ/kg)
m_{coal}	coal input mass flow (kg/s)
$\dot{m}_{oc}$	actual oxygen carrier circulation rate (kg/s)
$\dot{m}_{oc,s}$	stoichiometric oxygen carrier circulation rate (kg/s)
NCV^0	solid fuels net calorific value (kJ/kg)
$\dot{n}_i$	component molar flow rate (mol/s)
P	pressure (Pa)
P_{ref}	reference pressure (101.325 kPa)
R	universal gas constant (8.31 J/mol K)
s	entropy (kJ/mol K)
s_0	entropy at the reference state (kJ/mol K)
T	temperature (K)
T_0	reference temperature (298 K)
Tol	default relative convergence tolerance
U_t	fuel utilization factor (–)
V_{ref}	reference cell voltage (0.7 V)
V_{SOFC}	SOFC voltage (V)
W_{ASU}	air separation unit power (kW)
W_{AUX}	auxiliary power consumption (kW)
$W_{COAL\cdot P}$	coal milling and handling power (kW)
$W_{CO_2\cdot COM}$	CO_2 compression power (kW)
$W_{CO_2\cdot EX}$	CO_2 expander power (kW)
W_{GT}	gas turbine power (kW)
$W_{SOFC\cdot AC}$	SOFC AC power output (kW)
$W_{SOFC\cdot DC}$	SOFC DC power output (kW)
W_{ST}	steam turbine power (kW)
w	moisture content of the solid fuel
X_i	calculated value in iteration
x_i	molar fraction (–)
η_e	plant net power efficiency (%)
$\eta_{ex,c}$	component exergy efficiency (%)
$\eta_{ex,system}$	system exergy efficiency (%)
$\eta_{inverter}$	DC–AC inverter efficiency (%)
η_{SOFC}	SOFC efficiency (%)
λ	oxygen carrier excess ratio (–)

Acronym

AC	alternate current
ASU	air separation unit
CCS	carbon capture and storage
CLC	chemical looping combustion
CLHG	chemical looping hydrogen generation
DC	direct current
HHV	higher heating value
HRSG	heat recovery steam generator
IGCC	integrated gasification combined cycle
LHV	lower heating value
MEA	monoethanolamine
SOFC	solid oxide fuel cell

need gaseous fuel, integrated gasification combined cycles (IGCC) can be used [6], where the coal is first converted into syngas in a gasifier, which is then used to fuel the gas turbine in the combined cycle. The processes in an IGCC are based on energy cascade utilization to maximize the energy and exergy efficiencies. The overall IGCC efficiency without carbon capture is estimated to be 36–42% [7]. If CO_2 capture is added, an energy penalty around 6–7% points will be imposed for conventional IGCC [7].

Solid oxide fuel cells (SOFC) are electrochemical direct energy conversion devices with high efficiency, and need high temperatures (600–1000 °C) for their operation because their electrolyte is inadequately conductive at lower temperatures. A SOFC produces electricity directly from fuel gases through electrochemical oxidation reactions rather than combustion [8]. Their operation at high temperatures and pressures provides an opportunity for using their exhaust gases for preheating the input fuel and air and to provide the heat source for gas and/or steam turbines to generate more power. Many studies have been made about the integration of SOFC with steam and combined cycles (e.g., [9–15]). In such systems the high temperatures allow the internal reforming of light hydrocarbon fuels, such as methane, propane and butane, within the anode, or external reforming upstream of the anode can be employed to use heavier hydrocarbons, such as gasoline, diesel, jet fuel (JP-8) or biofuels [16]. The reformates are generically syngas, mixtures of hydrogen, carbon monoxide, carbon dioxide, steam and methane. The syngas then reacts in the fuel cells to produce electricity [17].

Since coal is a very abundant fossil fuel, especially in high-energy consuming countries like China and India, and SOFC has potential to attain efficiencies of around 60%, significant attention was given to use SOFC for replacing or augmenting the gas turbine power output in IGCC plants to attain higher overall efficiency of coal power plants [18,19]. The system of combining SOFC and IGCC is usually as follows: coal is gasified to syngas in a gasifier and cleaned, fed to the SOFC that produces power, the SOFC exhaust gases are mixed and burned in a combustor, and then fed to a gas turbine, producing additional power, the gas turbine exhaust flows into a heat recovery steam generator (HRSG). The steam is fed to the steam turbine for additional power generation. Romano et al. [20,21] performed a thermodynamic analysis of integrated gasification fuel cell plants. A simple cycle gas turbine works in a hybrid cycle with a pressurized intermediate temperature SOFC, integrated with coal gasification with a syngas cleanup island and a bottoming steam cycle, but without CO_2 capture. A net electric efficiency of 52–54% was predicted. El-Emam et al. [22] examined an integrated gasification and SOFC system with a combined cycle. The energy efficiency of the overall system was predicted to reach 38.1% without carbon capture. The influences of pressure ratio on the component performance were also presented in their study. Adams et al. [23] proposed an integrated gasification-SOFC power plant, with separated anode and cathode streams. Air is used as oxygen source without diluting the fuel exhaust, enabling CO_2 recovery from the exhaust with a very small energy penalty. The optimization process predicted that 46% power

efficiency could be achieved. In an analysis that included careful consideration of gas cleaning, Prabu and Jayanti [24] combined underground coal gasification with SOFC, taking advantage of the high temperature exhaust of SOFC to reform the syngas for hydrogen production. A detailed energy analysis of this system showed more than 4% thermal efficiency gain and 6% lower CO_2 emissions, compared with a conventional steam turbine cycle.

In this study, to the best of our knowledge the first to propose a novel integrated IGCC-SOFC plant that uses the emerging technology chemical looping combustion (CLC) process for more thermodynamically reversible and thus more efficient fuel conversion, and which also allows inherent CO_2 separation [25–29]. The CLC is comprised of two reactors: a fuel reactor and an air reactor. Instead of reacting fuel with oxygen directly, an oxygen carrier is reduced by the fuel and then re-oxidized by reaction with oxygen (usually supplied in air). Usually a metal oxide Me_xO_y, typically a transitional element, is used as the oxygen carrier. In the fuel reactor, this oxygen carrier is at a higher state and is reduced by the gaseous fuels. With the complete conversion of the fuel gases, the gas products are CO_2, H_2O vapor and the solid reduced metal oxide at a lower state Me_xO_{y-1}:

$$(2n+m)Me_xO_y + C_nH_{2m} \rightarrow (2n+m)Me_xO_{y-1} + mH_2O + nCO_2 \quad \Delta H < 0 \text{ or } > 0 \tag{1}$$

The CO_2 in the reaction products can be easily separated, by condensing the H_2O and removing the solid metal oxide particles by gravity and filtration. The reduced oxygen carrier at the lower state Me_xO_{y-1} enters the air reactor, and is re-oxidized to the higher state Me_xO_y by oxygen in the air:

$$Me_xO_{y-1} + 1/2O_2 \rightarrow Me_xO_y \quad \Delta H > 0 \tag{2}$$

where ΔH is the enthalpy of reaction. CLC can be also integrated with the natural gas combined cycle or coal gasification for power generation [30,31]. Naqvi et al. [32] presented an application of CLC method in natural gas-fired combined cycles for power generation with CO_2 capture. Reheating was introduced by employing multi CLC-reactors. The cycle was predicted to achieve net plant efficiency of above 51% including 100% CO_2 capture and compression to 110 bar. Petrakopoulou et al. [33] conducted an exergoeconomic analysis of a natural gas combined cycle power plant with chemical looping technology. The plant exergetic efficiency was predicted to reach 51.3%. For comparison, their conventional natural gas combined cycle without CO_2 capture was 56.3%, with monoethanolamine (MEA) for CO_2 capture efficiency is 45.8%. Erlach et al. [34] integrated CLC and IGCC, the performance of various configurations of CLC used in IGCC were analyzed and compared to the conventional IGCC design with pre-combustion carbon capture by physical absorption. It was found that the CLC-IGCCs offered the advantage of higher plant efficiency and more complete carbon capture. The predicted CLC-IGCC efficiency was 37.7–38.8% with near-zero carbon emission while the pre-combustion IGCC showed a maximum efficiency of 36.2% with minimum carbon emission of 123.82 kg/Mh_{el}. Chen et al. [35] incorporated a chemical looping hydrogen generation (CLHG) process within the SOFC. The chemical looping hydrogen generation process produced hydrogen and separated CO_2. The hydrogen was fed to the SOFC. The predicted net power efficiency was up to 43%, including CO_2 capture.

The main innovation in our study presented in this paper is that a SOFC and CLC are integrated with coal gasification for higher efficiency power generation with low CO_2 capture energy penalty (Fig. 1), with the process proceeding as follows:

(1) Coal is fed into the gasifier.
(2) The produced syngas fuels the SOFC that generates electrical power.
(3) The SOFC effluent gas containing CO_2, H_2O and some unconverted combustible fuel is fed to CLC reactor vessels for full fuel conversion and inherent CO_2 separation.
(4) The exhaust streams from CLC reactors enter the gas turbines that generate power.
(5) The exhausts from these turbines enter into a heat recovery steam generator (HRSG) to generate steam.
(6) The steam is fed to a steam turbine to generate more power.

2. System process

The flowsheet of the combined cycle plant is shown in Fig. 1. It includes five blocks: gasification, SOFC, chemical looping combustion, gas turbine and steam cycle, and CO_2 recovery and compression.

2.1. Gasification

A bituminous coal is gasified in a commercial dry-fed type gasifier using O_2 from an air separation unit (ASU). The ASU is assumed to produce 95 vol.% O_2 for the gasifier, with 4 vol.% Ar and 1 vol.% N_2. The studied plant is already a complicated system, so an analysis of the ASU is not incorporated here, but its specific power demand, 0.325 kW h/kg O_2 [21], is accounted for. The coal analysis is shown in Table 1. CO_2 rather than steam vapor is used as the gasification agent because CO_2 is separated and available from the CO_2 compression process downstream.

Oxygen and carbon dioxide ratio adopted is to just meet the requirements of coal combustion to provide sufficient heat for full coal gasification. This ratio may be varied as needed for different coals. In this work, the oxygen/coal mass ratio was assumed to be 0.9, and the CO_2/coal mass ratio was assumed to be 0.113 [35]. High temperature (1371 °C) and pressure (30.4 bar) are used in the gasifier at thermodynamic and chemical equilibrium. The hot syngas is quenched to 900 °C by recycling a portion of cooled syngas (350 °C). The syngas flows downstream into the waste heat boiler, where gas cooling is achieved by preheating the clean syngas for the SOFC and generating high pressure steam. After gas cleaning and sulfur removal, the syngas returns to the tubes in the waste heat boiler. It is preheated to a temperature of 800 °C before entering the SOFC stacks.

2.2. The SOFC

The SOFC is an electrochemical energy conversion device that produces electricity directly from oxidizing a fuel. The electrochemical conversion process in SOFC stacks accomplishes fuel oxidation in a more reversible way than the traditional combustion process. The electrical efficiency of SOFC is typically 40–60%. In this plant, the SOFC unit uses the syngas produced from the coal gasifier. In addition to the hydrogen produced in the gasifier, and the other produced fuel components like CH_4 and CO are converted to hydrogen using the available H_2O in the syngas within the cell stacks before electrochemical reactions:

$$\text{Steam reforming}: \ CH_4 + H_2O \leftrightarrow CO + 3H_2 \quad \Delta H = 206.172\,\text{kJ/mol} \tag{3}$$

$$\text{Water gas shift}: \ CO + H_2O \leftrightarrow CO_2 + H_2 \quad \Delta H = -41.169\,\text{kJ/mol} \tag{4}$$

The steam reforming reaction is endothermic. The heat required by the endothermic reaction is supplied by the heated cell stacks. The steam reforming reaction and the water gas shift reaction are thermodynamically favored because the hydrogen is continuously removed by electrochemical reactions. Hence, only hydrogen is assumed to be the anode input and react there electrochemically with oxygen ions.

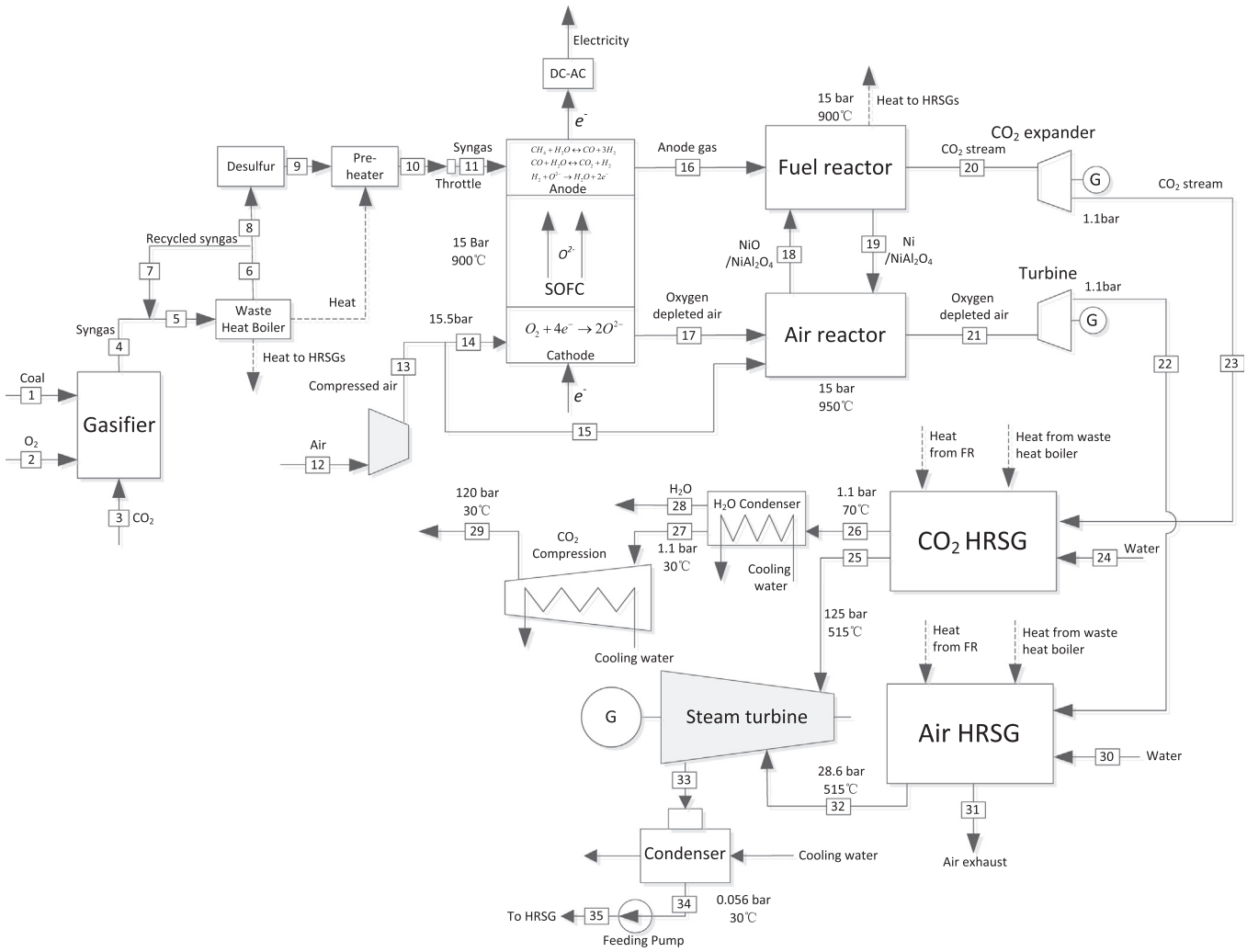

Fig. 1. The flowsheet of the proposed power plant integrating coal gasification, SOFC, CLC and combined power cycle.

Table 1
Analysis of the bituminous coal used.

Proximate analysis/% (mass, air dry)		Ultimate analysis/% (mass, air dry)	
Moisture	5.0	C	66.07
Volatile	39.24	H	5.07
Fixed carbon	46.26	O	9.5
Ash	9.5	N	1.19
		S	3.67
Lower heating value (LHV) = 26805 kJ/kg			
Higher heating value (HHV) = 27912 kJ/kg			

The electrochemical reactions that occur at the anode and the cathode of SOFC are:

$$\text{Anode}: \quad H_2 + O^{2-} \rightarrow H_2O + 2e^- \tag{5}$$

$$\text{Cathode}: \quad O_2 + 4e^- \rightarrow 2O^{2-} \tag{6}$$

The electrons produced at the anode side are directed to the cathode side and reacted with the oxygen molecules. The oxide ions produced from the cathode side diffused to the anode via the electrolyte layer. The electrolyte layer acts as a highly selective membrane for the oxygen transport from air to the fuel.

The amount of fuel reacted in the fuel cell was calculated, and also used in U_t, the fuel utilization factor, defined in Eq. (7). The unreacted H_2 and CO, as well as the remaining CH_4, CO_2 and H_2O, exit the cell stacks.

$$U_t = \left(\dot{n}_{H_2} + \dot{n}_{CO} + 4\dot{n}_{CH_4}\right)_{reacted} / \left(\dot{n}_{H_2} + \dot{n}_{CO} + 4\dot{n}_{CH_4}\right)_{input} \tag{7}$$

The SOFC temperature is 800–900 °C and the anode inlet fuel temperature is 800 °C. The cell voltage is an important parameter that determines the cell performance. The cell voltage depends on various parameters such as temperature, pressure, current density and geometric configuration. The cell voltage can thus be assigned only after the cell design specifications are determined. Since this study does not consider a specific fuel cell design, a simplified correlation approach is adopted. The cell voltage can be predicted as a function of cell temperature and pressure [36,37]:

$$V_{SOFC} = V_{ref} + \Delta V = V_{ref} + (RT/4F)\ln(P/P_{ref}) \tag{8}$$

V_{ref} is the reference cell voltage at a nominal design condition (800 °C, 3.5 bar), 0.70 V; R is the universal gas constant, 8.31 J/mol K; T is the fuel cell operating temperature, K; F is the Faraday constant, 96486 C/mol; P is the fuel cell operating pressure, bar and P_{ref} is the reference pressure, 3.5 bar.

The power (DC) generated by the fuel cell is calculated as follows:

$$W_{SOFC\text{-}DC} = V_{SOFC} I = V_{SOFC}\left(\dot{n}_{H_2} + \dot{n}_{CO} + 4\dot{n}_{CH_4}\right)_{reacted} 2F \tag{9}$$

The actual alternate current (AC) power production from the SOFC unit is calculated by:

$$W_{SOFC\cdot AC} = W_{SOFC\cdot DC}\ \eta_{inverter} \tag{10}$$

$\eta_{inverter}$ is the efficiency of the DC–AC inverter and assumed to be 95% [38].

The SOFC power efficiency is calculated by:

$$\eta_{SOFC} = \frac{W_{SOFC,AC}}{\dot{n}_{H_2,reacted}\mathrm{LHV}_{H_2} + \dot{n}_{CO,reacted}\mathrm{LHV}_{CO} + \dot{n}_{CH_4,reacted}\mathrm{LHV}_{CH_4}} \tag{11}$$

where LHV_{H_2}, LHV_{CO}, and LHV_{CH_4} are the lower heating value of H_2, CO and CH_4, respectively.

2.3. Chemical looping combustion (CLC)

A chemical looping combustor is deployed at the exhaust of the SOFC. The CLC is comprised of a fuel reactor and an air reactor. The anode effluent of SOFC contains unconverted syngas. The syngas stream is fed to the fuel reactor for completing the fuel conversion and reducing the oxygen carrier. The outlet stream from the fuel reactor is primarily CO_2 and H_2O. The reduced oxygen carrier enters the air reactors for re-oxidation. The cathode effluent of the SOFC, composed of oxygen and nitrogen flows to the air reactor for oxygen carrier regeneration. Additional air may be injected from the compressors for full oxidization of the reduced oxygen carrier. Oxygen carriers commonly used in CLC are transitional metal oxides, such as NiO, Fe_2O_3 and CuO. The pure metal oxide is prone to agglomerate and sinter after several cycles. To improve the activity against risk of agglomeration and sintering, the oxygen carrier is usually supported with an inert, which is a material combined with oxygen carrier by mechanical mixing, precipitation or impregnation methods. In this work, the inert supports for NiO, Fe_2O_3 and CuO are $NiAl_2O_4$, $FeAl_2O_4$ and Cu_2AlO_4, respectively [39]. The molar fraction of the oxygen carrier to its inert support is assumed to be 0.25. The excess ratio of an oxygen carrier (λ, Eq. (12)) is defined as the difference between the actual circulation rate of oxygen carrier and the stoichiometric circulation rate of oxygen carrier required for full fuel conversion, divided by that stoichiometric circulation rate. Here, $\lambda = 0.2$ is adopted for complete fuel conversion.

$$\lambda = \frac{\dot{m}_{oc} - \dot{m}_{oc,s}}{\dot{m}_{oc,s}} \tag{12}$$

$\dot{m}_{oc}$ is the actual circulation rate of oxygen carrier; $\dot{m}_{oc,s}$ is the stoichiometric circulation rate of oxygen carrier required for full fuel conversion.

2.4. The gas turbine and steam cycle

In this combined system, the SOFC stack and CLC reactor combination act as the combustor of the gas turbine cycle. The exhaust stream from the air reactor is at high temperature and pressure and directed to the air turbine. The air turbine could be connected with the air compressor on a single shaft. The CO_2-rich effluent stream from the fuel reactor flows to the CO_2 expander for additional power generation. The steam cycle mainly consists of an air HRSG, a CO_2 HRSG and a steam turbine. The gasifier, waste heat boiler and fuel reactor are all integrated with the air and CO_2 HRSGs for steam generation. Heat exchangers in the plant include economizers, evaporators, superheaters and reheaters. The steam enters the high pressure steam turbine and then is reheated in the waste heat boiler. Because the heat balance in the system changes depending on the units in the plant, the HRSG may be redesigned for some of the simulated cases to keep the same steam temperature and pressure.

2.5. CO_2 recovery and compression

The CO_2-rich gas from the CO_2 HRSG is cooled in a heat exchanger to 30 °C. The H_2O vapor is condensed there, which thus also separates the CO_2 (noncondensable gas) from the water. The resulting CO_2 stream is then compressed to 120 bar in a four-stage intercooled compressor, cooled using environmental water in each stage. The majority of water remaining in the CO_2 stream is removed in the flash drums of each compressor stage. The dehydrated CO_2 stream is then totally condensed for removal.

3. The analysis methodology

The components within the plant system are modeled as lumped control volumes, and their detailed component configurations are not considered. The plant system performance is first evaluated by the thermal efficiency, i.e., the plant net power efficiency, based on the first law of thermodynamics. The plant net power efficiency is the ratio of the net power output divided by the entire energy input. For this combined cycle plant, the net power efficiency of the plant is defined by:

$$\eta_e = \frac{W_e}{m_{coal}\cdot \mathrm{LHV}_{coal}} \times 100\% \tag{13}$$

where η_e represents the plant net power efficiency, %, which is also called thermal or electrical efficiency; m_{coal} represents the input coal mass flow, kg/s; LHV_{coal} represents the coal lower heating value, kg/kg.

The plant net power output is expressed as the following equation:

$$W_e = W_{SOFC\cdot AC} + W_{GT} + W_{ST} + W_{CO_2\cdot EX} - W_{COAL\cdot P} - W_{ASU} - W_{CO_2\cdot COM} - W_{AUX} \tag{14}$$

where $W_{SOFC\cdot AC}$ represents the SOFC AC power, kW; W_{GT} represents the gas turbine power, kW; W_{ST} represents the steam turbine power, kW; $W_{CO_2\cdot EX}$ represents the CO_2 expander power, kW; $W_{COAL\cdot P}$ represents the coal milling and handling power, kW; W_{ASU} represents the air separation unit power, kW; $W_{CO_2\cdot COM}$ represents the CO_2 compression power, kW; W_{AUX} represents the auxiliary power consumption, such as water recirculation pumps and blowers, kW.

Exergy is the maximum theoretical work available from a thermal system, when it is brought reversibly into equilibrium with a reference environment [40]. The exergy analysis is based on the second law of thermodynamics. The exergy of a system $\dot{e}_s$ can be separated into four parts: chemical, physical, kinetic and potential. The kinetic and potential exergy are relatively very small and thus neglected here, so the molar exergy of a system is:

$$\dot{e}_s = \dot{e}_{ch} + \dot{e}_{ph} \tag{15}$$

$\dot{e}_{ch}$ is the specific chemical exergy of different species in one molar mixture, kJ/mol; and can be written as follows:

$$\dot{e}_{ch} = \sum_{i=1}^{i=n} x_i e_{ch,i} + RT_0 \sum_{i=1}^{i=n} \ln x_i \tag{16}$$

where $e_{ch,i}$ is the specific standard molar chemical exergy of a substance at the reference state, kJ/mol; x_i is the molar fraction of each substance i; T_0 is the reference temperature, K. The specific molar physical exergy of a system is obtained from:

$$\dot{e}_{ph} = \sum_{i=1}^{i=n} x_i (h - h_0) - T_0 \sum_{i=1}^{i=n} x_i (s - s_0) \tag{17}$$

where h and s are the specific enthalpy and entropy of a substance at a given state, kJ/mol and kJ/mol K; h_0 and s_0 are the specific

enthalpy and entropy of a substance at the reference state, kJ/mol and kJ/mol K.

The total exergy of a stream is calculated by multiplying the specific exergy and the molar flow rate $\dot{n}$, mol/s.

$$\dot{E}_s = \dot{n}\dot{e}_s \tag{18}$$

Energy is conserved in thermodynamic process, but exergy is not conserved and can be destroyed due to losses. For a component, the exergy destruction is given by:

$$\dot{E}_{s,d} = \dot{E}_{s,i} - \dot{E}_{s,o} \tag{19}$$

$\dot{E}_{s,d}$ is the exergy destruction rate, kW, which is mainly caused by chemical reactions, heat exchange, friction and mixing; $\dot{E}_{s,i}$ is the inlet or input exergy flow rate, kW, and $\dot{E}_{s,o}$ is the outlet or product exergy flow rate, kW.

The exergy efficiency of the overall system $\eta_{ex,system}$ is following:

$$\eta_{ex,system} = \frac{E_P}{E_F} = 1 - \frac{E_D}{E_F} \tag{20}$$

E_P is the exergy product obtained in the system, kW; E_F is the fuel input exergy into the system, kW; E_D is the exergy destruction in the system, kW.

The exergy efficiency of a specific component in the system $\eta_{ex,c}$ is following:

$$\eta_{ex,c} = \frac{E_{output}}{E_{input}} \tag{21}$$

E_{output} is the exergy output of a component, kW; E_{input} is the exergy input of a component, kW.

In this work, coal is used as the fuel. The chemical exergy of coal is calculated based on the following formula which is commonly used for solid fossil fuels [40]:

$$e_{fuel} = [NCV^0 + 2442w]\varphi_{dry} + 9417s \tag{22}$$

NCV^0 represents the net calorific value of solid fuels, kJ/kg; w represents the moisture content of the solid fuel; s represents the mass fraction of sulfur in the solid fuel; φ_{dry} is expressed as the following [40]:

$$\varphi_{dry} = 1.0437 + 0.1882\frac{h}{c} + 0.0610\frac{o}{c} + 0.0404\frac{n}{c} \tag{23}$$

where c, h, o and n are the mass fractions of C, H, O and N elements in the solid fuel, respectively. This formula is applicable to a wide range of solid fuels with a mass ratio of O/C less than 0.667. The exergy analysis is very useful to determine where in the plant exergy is lost due to irreversible processes, which can then be considered for improvements.

The Aspen Plus software [41] was used for the plant system analysis. Solids processing was selected in the simulation. The Peng–Robinson equation of state with the Bostion–Mathias modification (PR–BM) was adopted as the property method for streams. ASME 1967 steam table corrections were used to calculate pure water and steam streams. The reactions in the gasifier, CLC reactors were calculated by RGibbs block, which uses Gibbs free energy minimization with phase splitting to reach equilibrium. RYield, which modeled a reactor where the reaction stoichiometry is unclear but the yield distribution was known, was added in the gasifier for pyrolysis. Heater and HeatX blocks were used for heat exchangers within the plant. All models or blocks were on the basis of mass and energy balance, and performed in a steady state and thermodynamic equilibrium. The kinetics of the reactions was thus not separately considered in this study.

In the Aspen Plus simulation, the default relative convergence tolerance *Tol* is 0.0001, which identifies whether the tear stream is converged or not. A tear is converged when the following is true for all tear convergence variables such as mole flow, pressure and enthalpy:

$$|(X_i - X_{i-1})/X_{i-1}| \leqslant Tol \tag{24}$$

X_{i-1} is the calculated value in iteration $i-1$; X_i is the calculated value in iteration i.

The primary component parameters are assumed and summarized in Table 2.

4. Results and discussion

4.1. Plant performance

Table 3 presents the performance of the proposed plant at a typical operating condition, using the assumption in Table 2:

Table 2
Essential simulation assumptions.

Air separation unit (ASU)	Oxygen purity, 95 vol.% (N_2, 4 vol.% and Ar, 1 vol.%) Oxygen pressure to gasifier, 36.5 bar [35] Specific work, 0.325 kW h/kg O_2 [21]
Coal milling and handling	0.022 kW h/kg [42]
Gasification process	Gasification temperature, 1371 °C [35] Pressure, 30.4 bar [35] Carbon conversion rate, 99% Oxygen/coal mass ratio, 0.90 [35] CO_2/coal mass ratio, 0.113 [35] Heat loss, 1% of input LHV Coal feed rate, 1 kg/s Gas quench type
Syngas quench and conditioning	Syngas temperature after quench, 900 °C Temperature of the quench gas, 350 °C Quench gas ratio, 49.2% Quench gas compressor efficiency, 75% Quench gas compressor ratio, 1.12
Heat exchangers in waste heat boiler	Pressure drop, 8% (2.4 bar) For clean syngas preheating, high pressure steam generation, reheating, intermediate pressure steam generation
Gas cleaning	Pressure drop, 6%
Solid oxide fuel cell (SOFC)	Operating temperature, 800–900 °C Pressure ratio, 5–20 Fuel utilization factor, 0.75–0.90 DC–AC converter efficiency, 95% [38]
Chemical looping combustion process	Oxygen carrier, NiO, inert support, $NiAl_2O_4$ Excess NiO coefficient, 0.2 $NiAl_2O_4$/NiO molar ratio, 0.25 Fuel reactor temperature, 850–950 °C Air reactor temperature, 850–950 °C Pressure, 5–20 bar
Air turbine (GT) and CO_2 expander	Discharge pressure, 110 kPa Isentropic efficiency, 90% Mechanical & generator efficiency, 98%
Heat recovery steam generator (HRSG)	Approach point, 10 °C Pinch point, 10 °C Pressure loss, 8%
Steam turbine cycle (Rankine)	Pressure levels, 12.5/2.86/0.4 MPa Intermediate pressure steam reheat Condenser pressure, 3.6 kPa Turbine isentropic efficiency, high pressure steam turbine 88%, intermediate steam turbine 92%, low pressure steam turbine 85% Mechanical and generator efficiency, 98%
CO_2 compression	Single stage compression ratio, 3.5 Compressor efficiency, 80% Mechanical and electrical efficiency, 98% CO_2 ready for pipeline, 30 °C, 120 bar [43]

Assumptions without references are explained in Section 2.

Table 3
Performance of the integrated system (SOFC temperature 900 °C, SOFC pressure 15 bar, fuel utilization factor U_t 0.85, fuel reactor temperature 900 °C, air reactor temperature 950 °C).

Coal LHV input, kW	26805 (1 kg/s)
Coal milling and handling power, $W_{COAL\cdot P}$, kW	79.2
ASU power, W_{ASU}, kW	1053.0
SOFC, $W_{SOFC\cdot AC}$, kW	7652.4
Gas turbine, W_{GT}, kW	2699.8
CO_2 expander, $W_{CO_2\cdot EX}$, kW	1469.8
Steam turbine, W_{ST}, kW	3729.1
CO_2 compressors, $W_{CO_2\cdot COM}$, kW	910.0 (1st 246, 2nd 254, 3rd 249, 4th 161)
Auxiliary power, W_{AUX}, kW	162.9
Plant net power efficiency (LHV), η_e%	49.8
CO_2 capture efficiency, %	~100

SOFC temperature 900 °C, SOFC pressure 15 bar, fuel utilization factor 0.85, fuel reactor temperature 900 °C and air reactor temperature 950 °C. The typical operating condition is just a baseline case but not the optimal one. The optimization of the system is done by the sensitivity analysis in the later section. Table 3 shows that the plant net power efficiency could reach 49.8%, including 100% CO_2 capture, which is more efficient and competitive than other alternative systems based on coal feeding. Table 4 presents the simulation results of the numbered flows shown in the flow diagram, Fig. 1.

Table 5 summarizes and compares the coal-fed power systems with CCS that were proposed and analyzed in past studies. Current supercritical coal-fired power plants without CCS have efficiencies approaching around 45% [62]. From Table 5, it is indicated that all coal gasification systems except [50,52] are reported to generate power at higher efficiency than those using oxy-fuel combustion or post-combustion CO_2 capture. Among gasification systems, IGCCs coupled with SOFC could offer higher efficiency. The oxy-fuel combustion efficiency is generally lower than that of gasification systems. The conventional pulverized coal plant with post-combustion capture usually shows the lowest efficiency, except if ultra-supercritical steam is used.

Compared with reference plants and with alternative capture technologies, the plant proposed in this work operates more efficiently (49.8% based on LHV, 47.8% based on HHV) and appears to be a thermodynamically promising approach for including carbon capture. The CO_2 capture rate could achieve ~100% compared with most of other plants in a range less than ~100%. The performance of the proposed plant is attractive because of predicted high power efficiency, low-to-zero CO_2 emissions and a potential investment cost saving. The reasons for the high efficiency of the proposed plant configuration are:

Table 4
Simulation results for selected flows of the typical case.

Flow no.	Type	Temperature (°C)	Pressure (bar)	Mass flow (kg/s)
1	Coal	35	30.5	1
2	Oxygen	150	36.5	0.9
3	CO_2	146.4	36.5	0.113
4	Syngas	1371	30.4	2.013
5	Syngas	900	28.8	3.779
6	Syngas	350	28.0	3.759
7	Syngas	367	31	1.848
8	Syngas	150	27	1.911
9	Syngas	340	27	1.762
10	Syngas	800	27	1.762
11	Syngas	800.4	15	1.762
12	Air	25	1.01	18.882
13	Air	424.5	15.5	18.882
14	Air	424.5	15.5	13.191
15	Air	424.5	15.5	5.691
16	Anode gases	900	15	2.642
17	Oxygen depleted air	900	15	12.312
18	$NiO/NiAl_2O_4$	950	15	2.541
19	$Ni/NiAl_2O_4$	900	15	2.263
20	CO_2 stream	900	15	2.919
21	Oxygen depleted air	950	15	17.725
22	Air exhaust	414.7	1.1	17.725
23	CO_2 stream	524.1	1.1	2.919
24	Water	30	0.056	1.153
25	Steam	540	125	1.153
26	CO_2 stream	70	1.1	2.919
27	CO_2 stream	30	1.1	2.919
28	Water	30	1.1	0.387
29	CO_2 stream	30	120	2.388
30	Water	30	0.056	2.092
31	Air exhaust	99	1.1	17.725
32	Steam	540	28.6	1.702
33	Steam exhaust	29.9	0.036	3.245
34	Water	29.9	0.036	3.245
35	Water	29.9	0.056	3.245

Table 5
Brief literature summary of coal-fed power system with CCS.

Researcher	System features	Efficiency	CO_2 capture
Rasul et al. [44]	Conventional coal power plant with post calcium carbonation carbon capture	35% (LHV basis)	~80%
Chmielniak et al. [45]	Supercritical coal power plant with amine absorption, using turbine steam to CO_2 desorption	45.20% (–)	85.5%
Liebenthal et al. [46]	Retrofitting post-combustion CO_2 capture process on steam power plant	34.55% (–)	90%
Ahn et al. [47]	Retrofitted MEA CO_2 capture in conventional power plant	28.8% (HHV basis)	90%
Romeo et al. [48]	$CaO–CaCO_3$ post combustion CO_2 capture in supercritical steam cycle	37.04% (LHV basis)	85%
Skorek-Osikowska et al. [49]	Oxy-combustion coal supercritical power unit	30.46–33.42% (LHV basis)	97.99%
Majoumerd et al. [50]	IGCC + Selexol + CO_2 capture	36.3% (LHV basis)	93.65%
Stadler et al. [51]	Oxy-fuel combustion with oxygen transport membranes	39.3–46.1% (LHV basis)	90%
Cormos et al. [52]	IGCC calcium-looping post-combustion capture; IGCC calcium-looping pre-combustion capture	34.22–37.02% (LHV basis)	95%
Kakaras et al. [53]	Oxyfuel application in lignite-fired power plant	32.29% (LHV basis)	90%
Perdikaris et al. [54]	Coal hydrogasification integrated with SOFC using CaO as CO_2 sorbent	40% (–)	90%
Nease et al. [55]	Coal gasification integrated SOFC with compressed air energy storage, oxy-anode fuel gas combustion for CO_2 capture	42.0% (HHV basis)	100%
Yan et al. [56]	Coal gasification + CaO absorption + SOFC	46.2% (LHV basis)	~100%
Kuchonthara et al. [57]	Thermochemical recuperative coal gasification integrated with fuel cell, membrane for CO_2 separation	45% (HHV basis)	~100%
Greppi et al. [58]	Coal gasification + MCFC (Molten Carbonate Fuel Cell)+GT combined cycle, no carbon capture	43% (HHV basis)	N/A
Kim et al. [59]	Coal gasification + SOFC + GT with pre-combustion or oxy-combustion (ITM for oxygen preparation)	37.5–46.6% (HHV basis)	95%
Siefert et al. [60,61]	IGCC-CCS with advanced H_2 and O_2 membrane; Catalytic gasification + SOFC with CO_2 sequestration; CaO-looping gasifier for IGFC-CCS and IGCC-CCS	43.4–58% (HHV basis)	70–100%
Reddy et al. [62]	Coal-fired supercritical thermal plant without CCS	43.5% (–)	N/A

'–' Do not indicate LHV or HHV basis.

(1) A SOFC theoretically produces electricity with higher efficiency than the commonly used conventional heat engines, such as gas turbines; the efficiency of SOFC η_{SOFC} is 53.2% in this work. Moreover, a SOFC plays a role of oxygen membrane and "separates" a portion of CO_2 by oxygen transfer through its electrolyte. The fraction of CO_2 separated within the cell is equal to the carbonaceous fuel utilization factor;
(2) CLC reactors are not only the combustors but also inherent CO_2 separators.

4.2. Exergy analysis

Exergy efficiency is defined as the ratio of exergy (available energy) output to total input exergy. Energy analysis does not properly indicate and quantify the losses caused by irreversibility, exergy analysis does, and it is most useful for discovering high exergy destruction subprocesses and for guiding ways to improve system performance.

Fig. 2 shows the Grassmann diagram of the entire plant. Table 6 indicates the exergy efficiency of the components calculated in this baseline plant along with defined inputs and outputs. In general, the SOFC exergy efficiency is defined as the ratio of product exergy over input exergy, but the inputs and products can be defined in different ways, especially for a component in the middle stream of the process. Two reasonable definitions including the resulting exergy efficiency value are listed in Table 6 for SOFC. The SOFC exergy performance is high regardless which definition is selected. The exergy efficiency of CLC reactors is high because the oxidation in them has low irreversibility (compared with conventional combustion) and because the high-temperature exhaust gas streams are valuable products for steam generation. The lowest exergy efficiency is found in the HRSG. The reason for the low exergy efficiency of HRSG is the relatively large temperature difference in heat transfer between hot and cold fluids, which indicates there is a potential improvement in heat exchanger layout.

The overall exergy efficiency can be calculated to evaluate the entire plant, and the performance of each component and its importance to the entire system can be assessed, by calculating the each exergy flow within the plant. Table 7 presents the exergy flows of the plant components. In Table 7, the exergy destruction is expressed as the difference between the inputs and outputs of the component. It can be seen that the gasifier contributes to the largest exergy destruction in the entire system, almost 33.91% of the total exergy loss within the plant, even though its exergy efficiency is higher than that of the HRSG. While the component exergy analysis is calculated just based on component input–output, it is known that the exergy destruction in the gasifier comes primarily from the coal and oxidization agents mixing, and the gasification process. The detailed sub-processes such as, solid–gas mixing, coal pyrolysis, char combustion, char gasification are not separately analyzed.

The second largest exergy destruction is in the CO_2 compression. The process includes the compression of CO_2 flue gas from the HRSG to a high pressure for transportation and storage. The separated pure CO_2 after the HRSG is intrinsically of high exergy because it was compressed to high pressure, exergy that may be lost if its sequestration method does not allow its use. The third highest exergy destruction is in the SOFC, 8.48%, the CLC reactors are the fourth, 7.04%. These destructions are moderate. While the gasification technology is commercially mature, the exergy destruction within it is very high, mostly because the combustion and gasification processes are irreversible exothermic processes, which do not produce work directly, but rather produce heat or syngas from which we generate work. Since chemical reactions are carried out irreversibly, a considerable part of the Gibbs energy change may not be utilized [63]. To maintain high overall system efficiency it is therefore important that the remaining energy conversion devices have high exergy efficiency. In our system an SOFC was chosen because it generates power efficiently and also enriches CO_2 in the anode side by transferring oxygen from cathode within its electrolyte. A CLC was chosen because it performs low-irreversibility fuel oxidation for the turbine and also provides inherent separation of CO_2 from the flue gas. No additional components and energy are thus needed for CO_2 separation, which also reduces the exergy destruction in the entire system.

Besides the gasifier, CO_2 compression, SOFC and CLC, 6.5% of the total exergy destruction of around 15745.87 kW, is lost in the gas cleaning, 4.86% in the gas turbine, 4.33% in the air separation unit, 4.19% in the HRSG, 3.42% in the steam turbine, 2.56% in the DC–AC inverter, and 2.35% in the air exhaust. These losses also underline the importance of these components performance.

4.3. Sensitivity analysis

4.3.1. SOFC temperature, pressure and fuel utilization factor

Fig. 3 presents the plant net power efficiency with the variation of the fuel utilization factor, SOFC temperature and SOFC pressure. The operating temperatures of the fuel reactor and the air reactor and consequently their outlet streams are constant at 900 °C and 950 °C, respectively, but the pressure of fuel reactor and air reactor would change due to variations of the upstream SOFC pressure.

The fuel utilization factor (U_t, Eq. (7)) is the gaseous fuel conversion rate in the SOFC stacks. In fact, the fuel utilization factor shares fuel gas fractions between the SOFC stacks and CLC reactor vessels. The fuel utilization factor is established by the SOFC intrinsic characteristics in the manufacturing process. It is technically difficult to change it during operation in an existing plant, so the different U_t values in Fig. 3 should be regarded as different SOFC design variants.

As shown in Fig. 3, increase of the fuel utilization factor leads to a higher plant net efficiency. If fuel utilization factor drops, more fuel is available for later turbines, but the net plant efficiency is still declining. At a fuel utilization factor 0.75, SOFC temperature 900 °C and a pressure 15 bar, the power outputs of SOFC, gas turbine and steam turbine are 6214.7 kW, 3063.53 kW and 4063.1 kW, respectively. With the same SOFC temperature and pressure, at a fuel utilization factor 0.90, the power output of SOFC is 8424.9 kW, increased by 35.6%; the power output of gas turbine is 2502.4 kW, decreased by 18.3% and the power output of steam turbine is 3552.9 kW, decreased by 12.6%. At a low fuel utilization factor in SOFC, more fuel is converted in the fuel reactor, generating more reduced oxygen carrier Ni. As the reduced Ni flows to the air reactor, more air is demanded to oxidize the reduced oxygen carrier to its original higher state NiO. At a fuel utilization factor 0.75, the mass flow of the air reactor outlet stream is 71234 kg/h, but it drops to 59781 kg/h (16.1% drop) at a fuel utilization factor 0.90. The decrease of mass flow from air reactor directly causes a drop in the power output of the gas turbine and the steam turbine downstream. That is why the SOFC power output increases but the gas turbine and the steam turbine power output decreases. The SOFC efficiency is 53.2% in the baseline case. It is more efficient than the conventional gas turbine cycle which is around 40%. More fuel converted in SOFC stacks, higher efficiency of the entire plant.

With raising of the SOFC temperature, the plant net power efficiency drops at a pressure around 5 bar whereas it rises above 5 bar. The power outputs of each component within the plant are compared in Fig. 4 with a fuel utilization factor of 0.85. According to Eq. (6), the SOFC voltage rises with the rise of temperature. With the same fuel utilization factor, SOFC generates more power. At a lower SOFC temperature, more air is needed to cool cell stacks to take away the heat released and maintain a

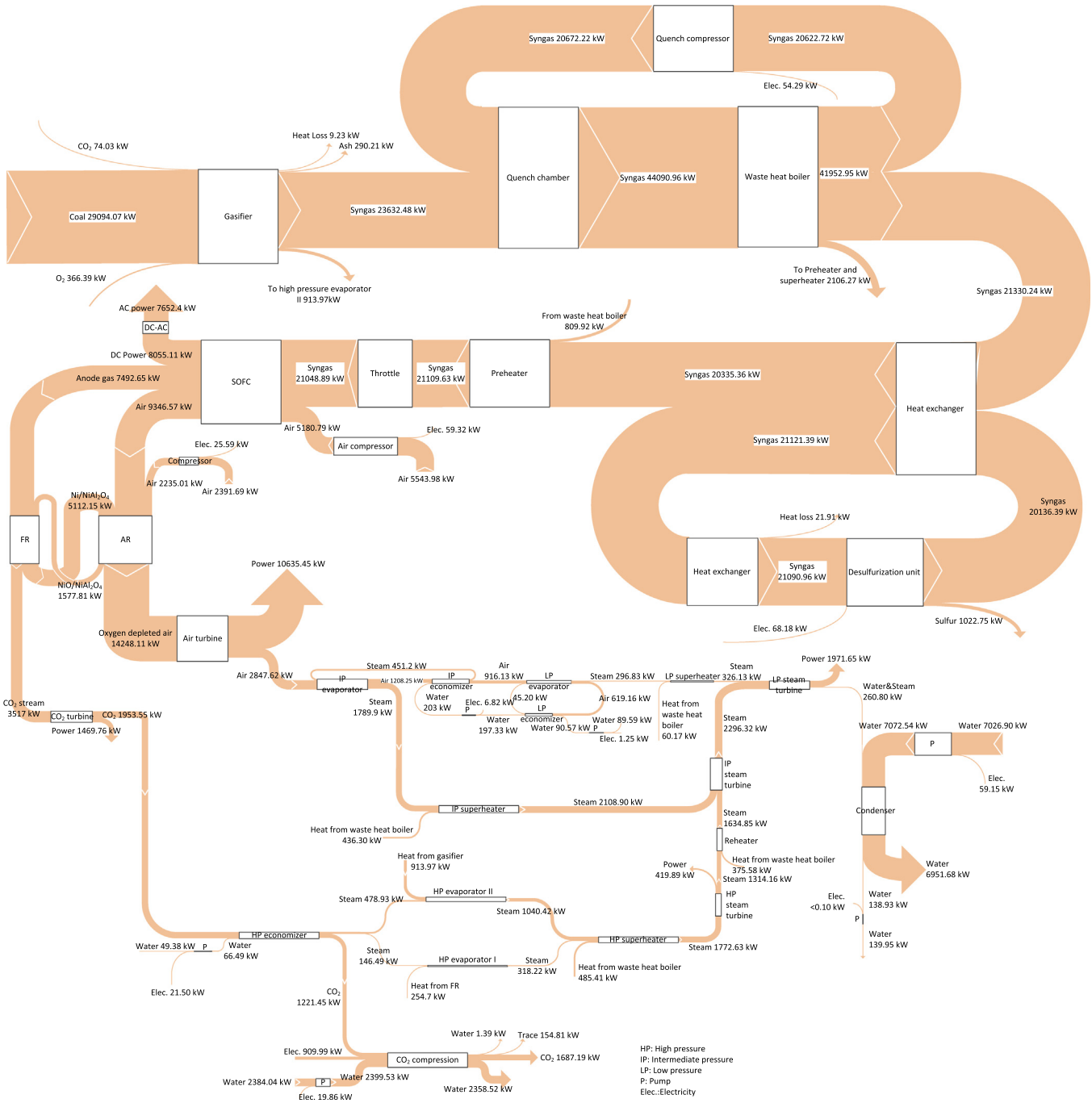

Fig. 2. Grassmann diagram of the entire plant.

constant SOFC operating temperature. Air into SOFC is supplied by the air compressor connected to the gas turbine. For the bottom cycle unit, i.e., gas turbine and steam turbine, the air increase required by SOFC leads to a decrease in the power output of gas turbine. More air from air reactor enters HRSG, generating more steam to drive the steam turbine. The power output of steam turbine increases accordingly. At a lower pressure of 5 bar, the decrease in the power output from gas turbine is higher than the increment in SOFC and steam turbine. The relatively poor performance of the gas turbine is because at a system pressure around 5 bar, the gas turbine greatly deviates from the optimal pressure ratio that is typically around 15 bar for our baseline case defined in Section 4.1. That is the reason why the plant net power efficiency decreases with the rise of SOFC temperature at a low pressure.

Fig. 3 also illustrates the impact of pressure on the plant net power efficiency. Raising the pressure is seen to increase the plant net power efficiency, but with diminishing returns. The plant achieves its highest net power efficiency at a pressure of 15 bar and then declines. It is similar to the tendency of a classical gas turbine cycle where at a constant gas turbine inlet temperature, raising the pressure first raises the power cycle efficiency, but with diminishing returns, until an optimal pressure (which offers the highest cycle efficiency), after which further increase of pressure results in an efficiency decline.

In this plant, the pressure influences the performance of the SOFC, steam turbine, gas turbine and CO_2 compressors significantly. As shown in Fig. 4, the power output of the SOFC increases monotonically with the rise of pressure because of the increase

Table 6
The computed exergy efficiencies of components from defined inputs and outputs.

Component	Exergy efficiency equation	Input	Output	Exergy efficiency, $\eta_{ex,c}$ (%)
Gasifier	$\frac{E_{syngas}+E_{steam}}{E_{coal}+E_{oxygen}+E_{CO_2}}$	Coal, oxygen, CO_2	Syngas, steam	82.22
Quench chamber	$\frac{E_{syngas,out}}{E_{syngas,in}}$	Syngas	Syngas	99.52
Waste heat boiler	$\frac{E_{steam,out}-E_{steam,in}}{E_{syngas,in}-E_{syngas,out}}$	Exergy decrease of syngas	Exergy increase of steam	87.42
SOFC	$\frac{E_{DC}+E_{air,out}+E_{syngas,out}+E_{steam}}{E_{syngas,in}+E_{air,in}}$	Syngas, air	DC power, air exhaust, flue gas, steam	94.90
	$\frac{E_{DC}+E_{air,out}-E_{air,in}+E_{steam}}{E_{syngas,in}-E_{syngas,out}}$	Exergy decrease of syngas	DC power, exergy increase of air, steam	90.15
DC–AC inverter	$\frac{E_{AC}}{E_{DC}}$	DC power	AC power	95.00
CLC	$\frac{E_{CO_2}+E_{air,out}+E_{steam,out}}{E_{SOFC,flue}+E_{air,in}+E_{steam,in}}$	SOFC flue gases, air, steam	CO_2 flue gas, air exhaust, steam	94.32
CO_2 expander	$\frac{E_{elec}}{E_{CO_2,in}-E_{CO_2,out}}$	Exergy decrease of CO_2 flue gas	Electricity	94.01
Air turbine	$\frac{E_{elec}}{E_{air,in}-E_{air,out}}$	Exergy decrease of air exhaust	Electricity	93.29
HRSG	$\frac{E_{steam,out}-E_{steam,in}}{E_{CO_2,in}-E_{CO_2,out}+E_{air,in}-E_{air,out}}$	Exergy decrease of CO_2 flue gas and air exhaust	Exergy increase of steam	79.47
Steam turbine	$\frac{E_{elec}}{E_{steam,in}-E_{steam,out}}$	Exergy decrease of steam	Electricity	87.38

in the hydrogen partial pressure. For the gas turbine, with the rise of inlet pressure, the power output increases but then decreases due to the compromise between the compressor power demand and the turbine power output. The CLC reactors act as combustors. The gas turbine inlet temperature is constant because the temperatures of the CLC reactors vessels are not changed. At the same turbine inlet temperature and a constant turbine exhaust pressure, the rise of inlet pressure creates a higher gas expansion ratio and lowers the exhaust temperature of the gas turbine. The exhaust stream from the gas turbine flows to the HRSG. The drop in the exhaust temperature of the gas turbine directly reduces the steam production rate of the HRSG and decreases the power output from the steam turbine. Therefore, the steam turbine power output diminishes with the increase of pressure.

The pressure has a strong influence on the power output of the CO_2 expander. The CO_2 expander exhaust is connected to the CO_2 HRSG. The CO_2 HRSG pressure is constant. So the CO_2 expander exhaust pressure is unchanged and therefore its power output is monotonically determined by its inlet pressure. After the reactions in gasifier, SOFC, CLC reactors, and CO_2 turbine, the carbon dioxide in the system is separated and ready for compression. The CO_2 expander exhaust pressure is not changed in all cases. The power consumed by the CO_2 compressors is therefore not influenced by the upstream pressure change.

It is noteworthy that the fuel utilization factor, SOFC temperature and SOFC pressure have small effect on the plant net power efficiency. This is because the SOFC is just one of the power production devices within the system. The other power generation components in the system include the gas and steam turbines. If the SOFC power decreases by varying the fuel utilization factor, the SOFC temperature or pressure, the gas turbine or the steam turbine will compensate the decreased power, as shown in Fig. 4. So in general, the influence of the fuel utilization factor, the SOFC temperature and pressure have small effect on the net power efficiency. This trend of parameter influence was also similar to other power unit systems. Jayanti et al. [64] investigated a high-temperature proton exchange membrane fuel cell unit integrated with ethanol reformer. The simulation results also revealed that the overall efficiency of the unit was not very sensitive to the operating temperature of cell stack or to the extent of hydrogen utilization.

4.3.2. Chemical looping combustion reactors temperatures

Fig. 5a illustrates the influence of the air reactor and fuel reactor temperature on the plant net power efficiency. The SOFC fuel utilization factor, temperature and pressure are kept the same while the reactor temperature changes. The SOFC fuel utilization factor is 0.85, the SOFC temperature is 900 °C and the pressure is 15 bar. The results show that with the rise of the air reactor temperature, the plant net power efficiency increases; but with the rise of the fuel reactor temperature, the plant net power efficiency decreases, with reasons explained as follows.

Since in this combined cycle plant, the CLC reactor vessels play a role of combustor in the conventional combined cycle, rise of the air reactor temperature raises the turbine inlet temperature and therefore increases the turbine's output power. The gas turbine exhaust temperature also increases and leads to an enhancement in the steam turbine power output. For example, in Fig. 5, at a fuel reactor temperature of 900 °C and an air reactor temperature of 850 °C, the power outputs of the gas turbine and the steam turbine are 3495 kW and 2394 kW, respectively. At the same fuel reactor temperature and an air reactor temperature of 950 °C, the power outputs of the gas turbine and the steam turbine are 3729 kW and 2680 kW, respectively, increased by 6.7% and 11.9%. The increase of air reactor temperature benefits the plant net power efficiency. The maximum temperature allowed is mainly dependent on the melting point and agglomeration risk of the oxygen carrier. 950 °C is typically used as the maximal temperature for NiO oxygen carriers air reactors [65–68].

Rise of the fuel reactor temperature causes the plant net power efficiency to drop. The nickel oxide reduction in the fuel reactor is exothermic, and the heat released by the fuel reactor is decreasing with the rise of reaction temperature. The fuel reactor is integrated with HRSG for steam generation. With the rise of fuel reactor temperature, less steam is generated in the HRSG. Even though the rise of fuel reactor temperature could increase CO_2 expander power, the total power output by the gas turbine and steam turbine is declining. So the rise of fuel reactor temperature leads to a drop in the net power efficiency.

In practice, the reduction reaction is relatively slow compared with the oxidation in the air reactor. A high fuel reactor temperature favors the reduction process of the oxygen carriers and is thus preferred. Thus the fuel reactor temperature is chosen as 900 °C in the baseline case of this study.

4.3.3. Different oxygen carriers

Besides NiO, many other oxygen carriers may be suitable for CLC, with much attention given to Fe_2O_3 and CuO, and their effects on the performance of the integrated system plant were also investigated in this study, with the results shown in Table 8. To make easier comparison, the SOFC block parameters, such as its temperature, pressure and fuel utilization factor are kept the same for all carriers. The CLC reactor temperatures when using Fe_2O_3 are the same as those using NiO (see results in Table 3), i.e. fuel reactor 900 °C and air reactor 950 °C. A change was made when

Table 7
Results of the exergy balance for each process element.

Component	$E_{x\text{-}in}$ streams involved	$E_{x\text{-}in}$, kW	$E_{x\text{-}out}$ streams involved	$E_{x\text{-}out}$, kW	$E_{x\text{-}des}$, kW	Percentage of total exergy destruction, %
Gasifier	1, 2, 3, 24	30013.42	4, 25	24672.90	5340.52	33.91
Quench chamber	4, 7	44304.70	5	44090.96	213.74	1.36
Waste heat boiler	5, 9, 24, 30	68889.03	6,10, 25, 32	68625.96	263.07	1.67
Ash Filter	8	41999.95	9	41952.95	47.00	0.30
Gas cleaning	8	21330.24	9	20335.36	994.88	6.32
Throttle	10	21109.63	11	21048.89	60.74	0.38
SOFC	11, 14	26229.68	16, 17, DC power	24894.33	1335.35	8.48
DC-AC inverter	DC power	8055.11	AC Power	7652.36	402.75	2.56
CLC reactors	15, 16, 17, 24, 30	19517.55	20, 21, 25, 32	18409.46	1108.09	7.04
CO_2 expander	20	3517.00	23, power	3423.31	93.69	0.60
Air turbine (GT)	21	14248.11	22, power	13483.07	765.04	4.86
HRSG	22, 23, 24, 30,	8401.69	25, 26, 31, 32	7742.57	659.12	4.19
Steam turbine	25, 32	8138.83	33, power	7600.41	538.42	3.42
CO_2 compression	26, power	2151.30	3	154.81	1996.49	12.68
Air compressor (GT)	12, power	8020.58	13	7415.80	604.78	3.84
Condenser	33, power	319.95	34	138.93	181.02	1.15
Auxiliary Pumps	6, 34, power	20747.89	7, 35	20738.71	9.18	0.06
ASU	Power	1053.00	–	366.39	681.61	4.33
Coal handling	Power	79.20	–	0	79.20	0.50
Air exhaust	31	371.18	–	0	371.18	2.35
					15745.87	100

Total exergy input, E_F, kW: 29094.07
Exergy output, E_P, kW: 13345.97
Total system exergy efficiency, $\eta_{ex,system}$, %: 45.87

Note: Fig. 1 is the simplified sketch map of the proposed system, so $E_{x\text{-}in}$ and $E_{x\text{-}out}$ streams in the table are just the streams involved in calculation. More details could be referred in Fig. 2.

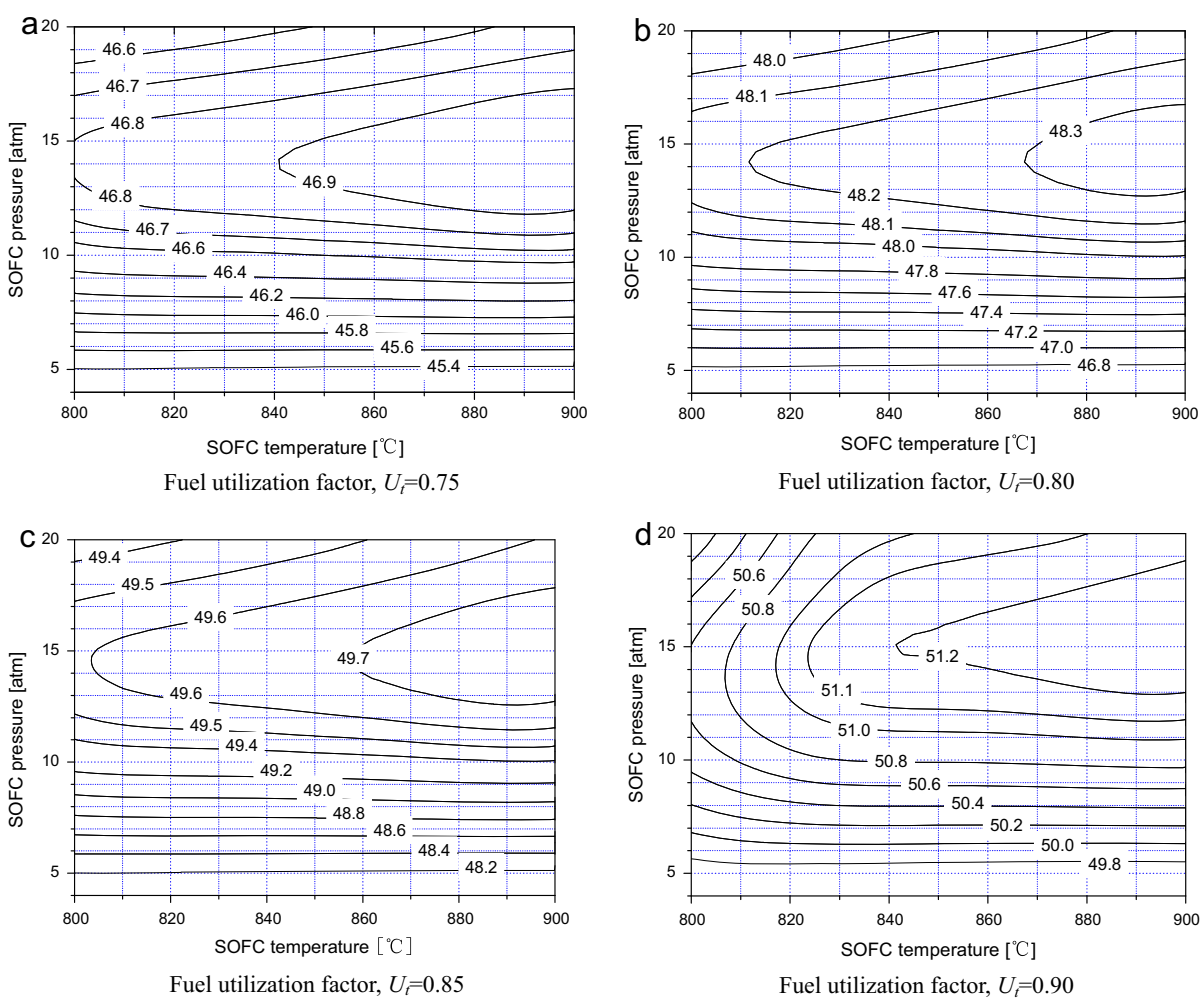

Fig. 3. The plant net power efficiency as a function of fuel utilization factor, SOFC temperature and pressure. (Fuel reactor and air reactor temperatures in CLC are kept constant at 900 °C and 950 °C, respectively.).

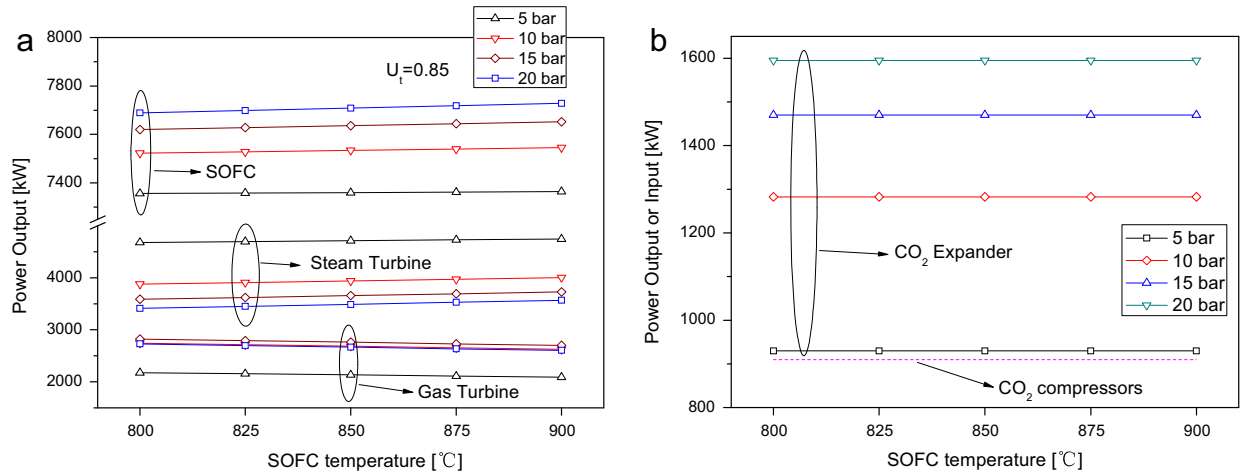

Fig. 4. The power output or input of the major components in the plant with the variation of SOFC temperature and pressure. (The fuel utilization factor is kept constant at 0.85, the fuel reactor temperature is 900 °C and the air reactor temperature is 950 °C.).

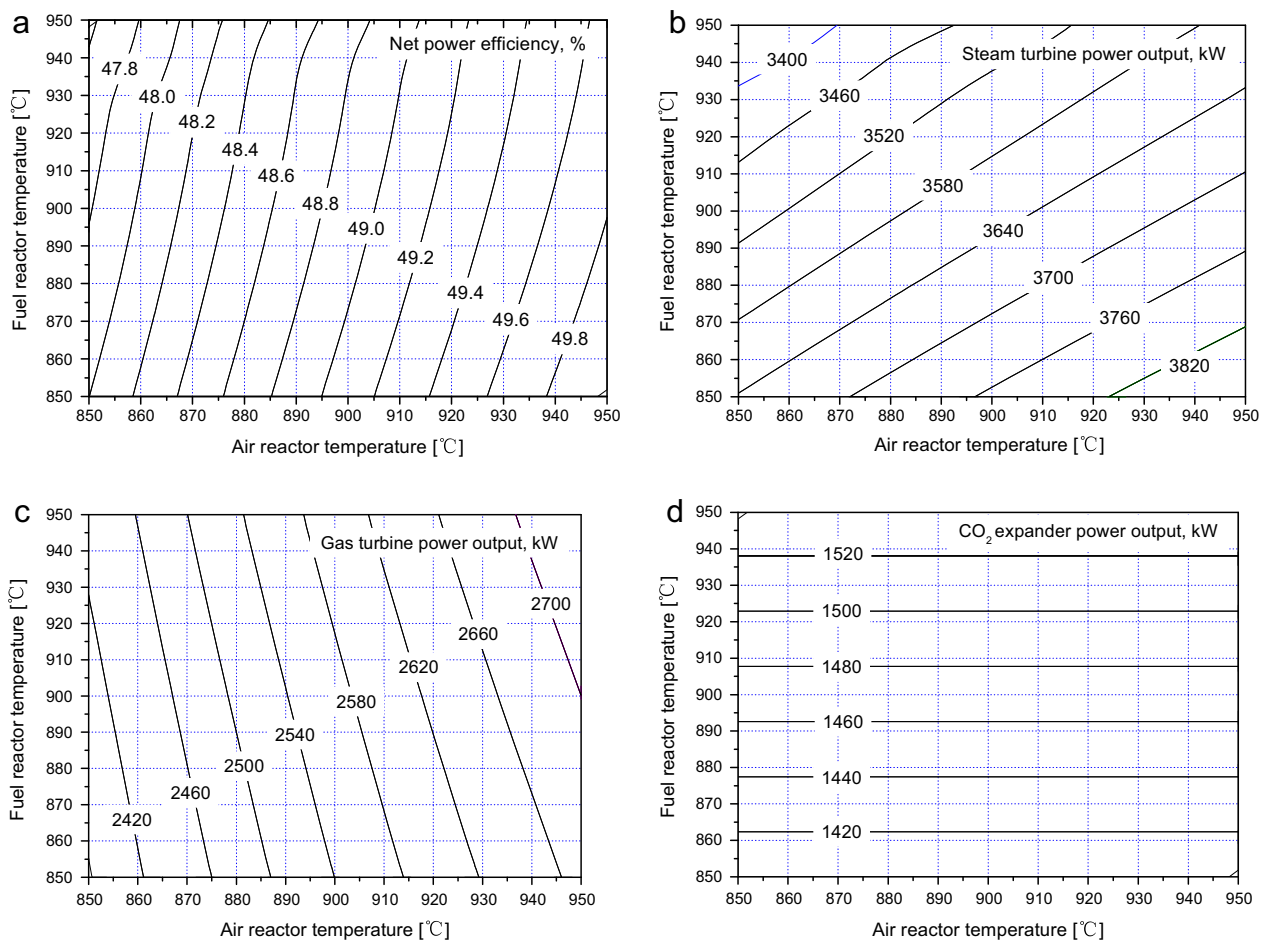

Fig. 5. The influence of the air reactor and fuel reactor temperature on the plant net power efficiency (SOFC fuel utilization factor 0.85, SOFC temperature 900 °C, pressure 15 bar).

CuO was used, because its particles tend to agglomerate at such high operating temperature due to the relatively low melting temperature of copper (1084 °C), by choosing 900 °C as the operating temperature for both the fuel and air reactors for this carrier.

In Table 8, it can be seen that the net power efficiency of the plant based on Fe_2O_3 oxygen carrier is 49.2%, which is slightly lower than that of the power plant based on NiO. The net power efficiency of CuO plant is obviously somewhat lower than the other two plants based on NiO and Fe_2O_3 due to lower CLC operating temperature permitted. Comparing NiO and Fe_2O_3 oxygen carriers, the gas turbine power output is higher for NiO while the steam turbine power output is higher for Fe_2O_3. This is primarily caused by the differences in heat release ratio between the fuel and air reactors among different oxygen carriers. The oxidation reaction of Ni

Table 8
Performance of the integrated plant using Fe_2O_3 and CuO as oxygen carriers.

	Fe_2O_3	CuO
Coal LHV input, kW	26805 (1 kg/s)	26805 (1 kg/s)
Coal milling and handling power, $W_{COAL\cdot P}$, kW	79.2	79.2
ASU power, W_{ASU}, kW	1053.0	1053.0
SOFC, $W_{SOFC\cdot AC}$, kW	7652.4	7652.4
Gas turbine, W_{GT}, kW	2355.8	2100.6
CO_2 expander, $W_{CO_2\cdot EX}$, kW	1470.5	1470.4
Steam turbine, W_{ST}, kW	3895.4	3748.1
CO_2 compressors, $W_{CO_2\cdot COM}$, kW	906.6	906.6
Auxiliary power, W_{AUX}, kW	147.2	173.5
Plant net power efficiency, η_e, %	49.2	47.6
CO_2 capture efficiency, %	~100	~100

to NiO releases more heat in the air reactor. Subsequently, more air is injected into the air reactor to keep a constant temperature, causing a larger mass flow rate and more power output from the gas turbine. At the same time, the heat released in the NiO fuel reactor is lower than that of Fe_2O_3. Thus, the steam production in HRSG decreases, resulting in a reduction in the power output of the steam turbine for the NiO oxygen carrier.

Besides superior net power efficiency with the NiO oxygen carrier, it has shown very high reactivity and is the most extensively analyzed one in the literatures [69] (all based on thermodynamic equilibrium, Gibbs function minimization). The disadvantage of the NiO oxygen carrier is the relatively low fuel conversion rate in the fuel reactor: in the reduction process 99.4% for CO and 99.5% for H_2 at 900 °C. The resulting trace combustible impurities not only impose a penalty in efficiency but also complicate the CO_2 compression and transportation process. Fe_2O_3 offers a higher fuel gas conversion rate in the CLC reactors. The CO_2 and H_2 conversion rate is more than 99.997%. CuO has the benefits of high fuel gas conversion rate (99.999%) and reaction kinetics, which favors the design of CLC reactors. Use of CuO oxygen carrier results, however, in lower plant net power efficiencies due to its above-mentioned temperature limitations.

4.4. Discussion

4.4.1. Challenges and opportunities

As described, the proposed system is comprised of gasification, SOFC, CLC, gas turbines and a steam power cycle. While there are some commercial IGCC plant demonstrations for power generation, there are none yet that are integrated even with SOFC alone, even though SOFC is technologically viable. This is primarily due to the prohibitive comparative cost of SOFC in large-scale plant unit [70]. Further, although SOFC has high flexibility to fuels, the fuel quality requirement for electrochemical reactions within a SOFC is more stringent than for conventional gas turbines. E.g., sulfur must be removed before the SOFC, and the CLC process downstream is also intolerant to sulfur.

CLC is also a technology under intense development but not mature yet and still needs large-scale demonstration and success for proof of practicality. An important challenge is attrition and activity loss of oxygen carriers over time. Another challenge is solid particles' separation before the gas streams from the CLC reactors enter the turbines, to avoid turbine blade fouling and erosion [71,72]. This separation problem has already been known in the development of pressurized fluidized bed combustion-combined cycle (PFBC-CC) years ago [73]. The CLC plant technology faces similar challenges in PFBC-CC.

In summary, integration of either SOFC or CLC alone with coal gasification already poses challenges, so including both into the proposed system would further complicate the situation. Furthermore it is nearly impossible at this stage of the proposed system development to perform its sensible economic analysis. While it is predicted in this study to have comparatively high energy efficiency with full CO_2 capture and thus offers a promising novel option to the world's critically needed approach to "clean coal", its practical realization depends on meeting the mentioned challenges, on maturity of SOFC and CLC independently, and on the system economics. The wide interest and activity in developing SOFC and CLC for many applications, and rate of progress of these systems, as well as the intense global interest in "clean coal", present an optimistic outlook for the future of the proposed system.

4.4.2. System advantages over IGCC with CO_2 separation

Conventional IGCC could pre-capture CO_2 by adding a process with the equipment needed for it to shift CO into CO_2 and then to separate the CO_2 by chemical or physical sorbents. Not only additional equipment is needed, but also heat is needed for the chemical or physical sorbents regeneration. The addition of the CO_2 removal units imposes investment cost and energy penalties in conventional IGCCs. In our proposed plant, CLC reactors substitute for the combustors in the gas turbine, and the CO_2 is intrinsically separated by the SOFC and CLC reactors. That is the ultimate reason why a high-efficiency is achieved in this plant.

Coal is the fuel used in our proposed plant, and it must be converted to syngas for the processes in the SOFC and CLC. Air could be used as the gasification agent, but the syngas produced by gasification will then contain a large amount of nitrogen, which will then get mixed into the CO_2 stream. So an ASU is indispensable in this plant to produce pure oxygen. In our system configuration we selected a typically-used cryogenic ASU to provide oxygen for coal gasification. We note that the capacity required for an ASU for gasification is smaller than that need for oxy-combustion plants, because a gasifier does not demand full coal combustion. Nevertheless, the energy consumed in the ASU in our system is still enormous; the ASU consumes 6.8% of the total power output within the plant and shares 47.8% fraction of the ancillary power.

It is noteworthy that a cryogenic O_2 separation process operates at high pressures and low temperature, which is the opposite of the attributes of the gasification in the process we analyzed, and may be replaced in the future by more efficient processes that are under development. For example, production of oxygen from air could be done by membrane separation processes, such as by ion transport membrane (ITM) that are predicted to have a higher efficiency [74]. ITM is operated at high temperature and generation of a pressure difference across the membranes (typ. 800–900 °C, and 14–20 bar on the air feed side and low to sub-atmospheric pressure on the oxygen permeate side), with energy recovery of the hot, pressurized, non-permeate stream by a gas turbine power generation system. Incorporation into our system could be by directing the stream of high temperature air after the SOFC or CLC to ITM for producing oxygen, which then is fed to the gasifier.

5. Conclusions

A novel combined cycle integrating coal gasification, solid oxide fuel cell, and chemical looping combustion was configured and analyzed. A thermodynamic analysis based on energy and exergy was performed to investigate the performance of the integrated system, determine the system components efficiency and to perform a sensitivity analysis of the system performance to the SOFC fuel utilization factor, SOFC temperature, pressure, fuel and air reactor temperature, and different oxygen carriers. The program subroutines and results were validated by comparison with available literature on similar systems. The major findings are:

- The system offers high energy efficiency with zero CO_2 emission: using NiO as oxygen carrier in the CLC unit, at the baseline case with SOFC temperature of 900 °C, SOFC pressure of 15 bar, fuel utilization factor 0.85, fuel reactor temperature 900 °C and air reactor temperature 950 °C, the plant net power efficiency is predicted to reach 49.8% (based on coal LHV), including the energy penalties for coal gasification, oxygen production, and CO_2 compression.
- Raising the SOFC temperature and fuel utilization factor raise the plant net power efficiency. At the baseline case, increase the SOFC temperature from 800 °C to 900 °C, the net power efficiency increases from 49.6% to 49.8%; increase the SOFC fuel utilization factor from 0.75 to 0.90, the net power efficiency increases from 47.0% to 51.3%.
- The SOFC power output increases with the raising of pressure. Raising the SOFC pressure up to a certain value, here 15 bar, raises the plant net power efficiency, but causes it to drop as the pressure is increased further, due to the compromise between the gas turbine output and the air compressor demand.
- Raising the CLC air reactor temperature raises the plant net power efficiency, but raising the fuel reactor temperature reduces that efficiency.
- The fuel utilization factor, the SOFC temperature and SOFC pressure have small effects on the plant net power efficiency because changes in pressure and temperature that increase the power generation by the SOFC tend to decrease the power generation by the gas turbine and steam cycle, and v. v. While simultaneous increase in the power generation of all three components would have been desirable, the characteristic of the system has an advantage: it maintains a nearly constant power output even when the temperature and the pressure vary.
- The largest exergy loss portion is in the gasification process, the second largest is in the CO_2 compression, and the third is in the SOFC.
- Compared with Fe_2O_3 and CuO oxygen carriers, NiO results in higher plant net power efficiency.

To the authors' knowledge, this is the first analysis synergistically combining in a hybrid system: (1) coal gasification, (2) SOFC, and (3) CLC, which results in a system of high energy efficiency with full CO_2 capture, and advances the progress to the world's critically needed approach to "clean coal".

Acknowledgements

The authors wish to express thanks to the National High Technology Research and Development Program of China (2012AA051801), the National Natural Science Foundation of China (51176033), the Foundation of Graduate Creative Program of Jiangsu (CXZZ-0147), and the Scholarship Award for Excellent Doctoral Student granted to the first author by the Ministry of Education and China Scholarship Council, which enabled him to spend a year as a visiting scholar at the University of Pennsylvania.

References

[1] Parikh J, Lior N. Energy and its sustainable development for India, editorial introduction and commentary to the special issue of energy-the international journal. Energy 2009;34:923–7.
[2] IEA Statics. CO_2 emissions from fuel combustion highlights; 2013 <http://www.iea.org/publications/freepublications/publication/CO2EmissionsFromFuelCombustionHighlights2013.pdf>.
[3] Yang Y, Guo X, Wang N. Power generation from pulverized coal in China. Energy 2010;35:4336–48.
[4] Guttikunda SK, Jawahar P. Atmospheric emissions and pollution from the coal-fired thermal power plants in India. Atmos Environ, http://dx.doi.org/10.1016/j.atmosenv.2014.04.057.
[5] Zhang N, Lior N, Jin H. The energy situation and its sustainable development strategy in China. Energy 2011;36:3639–49.
[6] US Department of Energy Report. Current and future IGCC technologies: a pathway study focused on non-carbon capture advanced power systems R&D using bituminous coal, vol. 1. DOE/NETL-2008/1337, August 2008.
[7] US DOE Report. Cost and performance baseline for fossil energy plants-volume 3a: Low rank coal to electricity: IGCC Cases. DOE/NETL-2010/1399, May 2011.
[8] Adams II TA, Nease J, Tucker D, Barton PI. Energy conversion with solid oxide fuel cell systems: a review of concepts and outlooks for the short- and long-term. Ind Eng Chem Res 2013;52:3089–111.
[9] Dunbar WR, Lior N, Gaggioli RA. The effect of the fuel cell unit on the efficiency of a fuel-cell-topped Rankine power cycle. J Energy Resour Technol 1993;115:105–7.
[10] Dunbar WR, Lior N. Combining fuel cells with fuel-fired power plants for improved exergy efficiency. Energy 1991;16:1259–74.
[11] Matelli JA, Bazzo E. A methodology for thermodynamic simulation of high temperature, internal reforming fuel cell system. J Power Sour 2005;142:160–8.
[12] Arsalis A. Thermoeconomic modeling and parametric study of hybrid SOFC-gas turbine–steam turbine power plants ranging from 1.5 to 10 MWe. J Power Sour 2008;181:313–26.
[13] Park SK, Ahn JH, Kim TS. Performance evaluation of integrated gasification solid oxide fuel cell/gas turbine systems including carbon dioxide capture. Appl Energy 2011;88:2976–87.
[14] Granovskii M, Dincer I, Rosen MA. Performance comparison of two combined SOFC-gas turbine systems. J Power Sour 2007;165:307–14.
[15] Najafi B, Shirazi A, Aminyavari M, Rinaldi F, Taylor RA. Exergetic, economic and environmental analyses and multi-objective optimization of an SOFC-gas turbine hybrid cycle coupled with an MSF desalination system. Desalination 2014;334:46–59.
[16] Bavarsad PG. Energy and exergy analysis of internal reforming solid oxide fuel cell-gas turbine hybrid system. Int J Hydrogen Energy 2007;32:4591–9.
[17] Petrakopoulou F, Lee YD, Tsatsaronis G. Simulation and exergetic evaluation of CO_2 capture in a solid-oxide fuel-cell combined-cycle power plant. Appl Energy 2014;114:417–25.
[18] Krüger M, Wörner A, Müller-steinhagen H. Solid oxide fuel cell (SOFC) hybrid power plant with integrated coal gasification: process variations and possible ways to separate carbon dioxide. Chem Ing Tech 2007;79:1323.
[19] Lisbona P, Romeo LM. Enhanced coal gasification heated by unmixed combustion integrated with a hybrid system of SOFC/GT. Int J Hydrogen Energy 2008;33:5755–64.
[20] Romano MC, Campanari S, Spallina V, Lozza G. Thermodynamic analysis and optimization of IT-SOFC-based integrated coal gasification fuel cell power plants. J Fuel Cell Sci Technol 2011;8:041001.
[21] Romano MC, Spallina V, Campanari S. Integrating IT-SOFC and gasification combined cycle with methanation reactor and hydrogen firing for near zero-emission power generation from coal. Energy Proc 2011;4:1168–75.
[22] El-Emam RS, Dnicer I, Naterer GF. Energy and exergy analyses of an integrated SOFC and coal gasification system. Int J Hydrogen Energy 2012;37:1689–97.
[23] Adams II TA, Barton PI. High-efficiency power production from coal with carbon capture. AIChE J 2010;56(12):3120–36.
[24] Prabu V, Jayanti S. Underground coal–air gasification based solid oxide fuel cell system. Appl Energy 2012;94:406–14.
[25] Ishida M, Jin H. A new advanced power-generation system using chemical-looping combustion. Energy 1994;19:415–22.
[26] Jin H, Ishida M. A new type of coal gas fueled chemical-looping combustion. Fuel 2004;83:2411–7.
[27] Lyngfelt A, Leckner B, Mattisson T. A fluidized-bed combustion process with inherent CO_2 separation; application of chemical-looping combustion. Chem Eng Sci 2001;56:3101–13.
[28] Jerndal E, Mattisson T, Lyngfelt A. Thermal analysis of chemical-looping combustion. Chem Eng Res Des 2006;84(A9):795–806.
[29] Tong A, Bayham S, Kathe MV, Zeng L, Luo S, Fan LS. Iron-based syngas chemical looping process and coal-direct chemical looping process development at Ohio State University. Appl Energy 2014;113:1836–45.
[30] Brandvoll Ø, Bolland O. Inherent CO_2 capture using chemical looping combustion in a natural gas fired power cycle. J Eng Gas Turbines Power 2004;126:316–21.
[31] Basavaraj BJ, Jayanti S. Syngas-fueled, chemical-looping combustion-based power plant lay-out for clean energy generation. Clean Technol Environ Policy 2014. http://dx.doi.org/10.1007/s10098-014-0781-0.
[32] Naqvi R, Bolland O. Multi-stage chemical looping combustion (CLC) for combined cycle with CO_2 capture. Int J Greenhouse Gas Control 2007;1:19–30.
[33] Petrakopoulou F, Boyano A, Gabrera M, Tsatsaronis G. Exergoeconomic and exergoenvironmental analyses of a combined cycle power plant with chemical looping technology. Int J Greenhouse Gas Control 2011;5:475–82.
[34] Erlach B, Schmidt M, Tsatsaronis G. Comparison of carbon capture IGCC with pre-combustion decarbonisation and with chemical-looping combustion. Energy 2011;36:3804–15.
[35] Chen S, Xue Z, Wang D, Xiang W. An integrated system combining chemical looping hydrogen generation process and solid oxide fuel cell/gas turbine cycle for power production with CO_2 capture. J Power Sour 2012;215:89–98.
[36] Park SK, Kim TS. Comparison between pressured design and ambient pressure design of hybrid solid oxide fuel cell-gas turbine systems. J Power Sour 2006;163:490–9.

[37] Yang WJ, Park SK, Kim TS, Kim JH, Sohn JL, Ro ST. Design performance analysis of pressured solid oxide fuel cell/gas turbine hybrid systems considering temperature constraints. J Power Sour 2006;160:462–73.
[38] Yi Y, Rao AD, Brouwer J, Samuelsen GS. Analysis and optimization of a solid oxide fuel cell and intercooled gas turbine (SOFC-ICGT) hybrid cycle. J Power Sour 2004;132:77–85.
[39] Hossain MM, de Lasa HI. Chemical-looping combustion (CLC) for inherent CO_2 separation-a review. Chem Eng Sci 2008;63:4433–51.
[40] Kotas TJ. The exergy method of thermal plant analysis. Malabar (FL): Krieger Publishing Company; 1995.
[41] Aspen Plus®, Version V7.2. Aspen technology <http://www.aspentech.com/>.
[42] Xiang W, Chen S, Xue Z, Sun X. Investigation of coal gasification hydrogen and electricity co-production plant with three-reactors chemical looping process. Int J Hydrogen Energy 2010;35:8580–91.
[43] Goto K, Yogo K, Higashi T. A review of efficiency penalty in a coal-fired power plant with post-combustion CO_2 capture. Appl Energy 2013;111:710–20.
[44] Rasul MG, Moazzem S, Khan MMK. Performance assessment of carbonation process integrated with coal fired power plant to reduce CO_2 (carbon dioxide) emissions. Energy 2014;64:330–41.
[45] Chmielniak T, Lepszy S, Wójcik K. Analysis of gas turbine combined heat and power system for carbon capture installation of coal-fired power plant. Energy 2012;45:125–33.
[46] Liebenthal U, Linnenberg S, Oexmann J, Kather A. Derivation of correlations to evaluate the impact of retrofitted post-combustion CO_2 capture processes on steam power plant performance. Int J Greenhouse Gas Control 2011;5:1232–9.
[47] Ahn H, Luberti M, Liu Z, Brandani S. Process configuration studies of the amine capture process for coal-fired power plants. Int J Greenhouse Gas Control 2013;16:29–40.
[48] Romeo LM, Abanades JC, Escosa JM, Paño J, Giménez A, Sánchez-Biezma A, et al. Oxyfuel carbonation/calcination cycle for low cost CO_2 capture in existing power plants. Energy Convers Manage 2008;49:2809–14.
[49] Skorek-Osikowska A, Bartela L, Kotowicz J, Job M. Thermodynamic and economic analysis of the different variants of a coal-fired, 460 MW power plant using oxy-combustion technology. Energy Convers Manage 2013;76:109–20.
[50] Majoumerd MM, De S, Assadi M, Breuhaus P. An EU initiative for future generation of IGCC power plants using hydrogen-rich syngas: simulation results for the baseline configuration. Appl Energy 2012;99:280–90.
[51] Stadler H, Beggel F, Habermehl M, Persigehl B, Kneer R, Modigell M, et al. Oxyfuel coal combustion by efficient integration of oxygen transport membranes. Int J Greenhouse Gas Control 2011;5:7–15.
[52] Cormos C, Cormos A. Assessment of calcium-based chemical looping options for gasification power plants. Int J Hydrogen Energy 2013;38:2306–17.
[53] Kakaras E, Doukelis A, Giannakopoulos D, Koumanakos A. Economic implications of oxyfuel application in a lignite-fired power plant. Fuel 2007;86:2151–8.
[54] Perdikaris N, Panopoulos KD, Fryda L, Kakaras E. Design and optimization of carbon-free power generation based on coal hydrogasification integrated with SOFC. Fuel 2009;88:1365–75.
[55] Nease J, Adams II TA. Coal-fuelled systems for peaking power with 100% CO_2 capture through integration of solid oxide fuel cells with compressed air energy storage. J Power Sour 2014;251:92–107.
[56] Yan L, He B, Pei X, Li X, Wang C. Energy and exergy analyses of a zero emission coal system. Energy 2013;55:1094–103.
[57] Kuchonthara P, Bhattacharya S, Tsutsumi A. Combination of thermochemical recuperative coal gasification cycle and fuel cell for power generation. Fuel 2005;84:1019–21.
[58] Greppi P, Bosio B, Arato E. Feasibility of the integration of a molten carbonate fuel–cell system and an integrated gasification combined cycle. Int J Hydrogen Energy 2009;34:8664–9.
[59] Park SK, Ahn JH, Kim TS. Performance evaluation of integrated gasification solid oxide fuel/gas turbine systems including carbon dioxide capture. Appl Energy 2011;88:2976–87.
[60] Siefert NS, Litster S. Exergy and economic analyses of advanced IGCC-CCS and IGFC-CCS power plants. Appl Energy 2013;107:315–28.
[61] Siefert NS, Chang BY, Litster S. Exergy and economic analysis of a CaO-looping gasifier for IGFC-CCS and IGCC-CCS. Appl Energy 2014;128:230–45.
[62] Reddy VS, Kaushik SC, Tyagi SK. Exergy analysis and evaluation of coal-fired supercritical thermal power plant and natural gas-fired combined cycle power plant. Clean Technol Environ Policy 2014;16:489–99.
[63] Leites IL, Sama DA, Lior N. The theory and practice of energy saving in the chemical industry: some methods for reducing thermodynamic irreversibility in chemical technology processes. Energy 2003;28:55–97.
[64] Jaggi V, Jayanti S. A conceptual model of a high-efficiency, stand-alone power unit based on a fuel cell stack with an integrated auto-thermal ethanol reformer. Appl Energy 2013;110:295–303.
[65] Mattisson T, Jerndal E, Linderholm C, Lyngfelt A. Reactivity of a spray-dried $NiO/NiAl_2O_4$ oxygen carrier for chemical-looping combustion. Chem Eng Sci 2011;66:4636–44.
[66] Jerndal E, Mattisson T, Thijs I, Snijkers F, Lyngfelt A. Investigation of $NiO/NiAl_2O_4$ oxygen carriers for chemical-looping combustion produced by spray-drying. Int J Greenhouse Gas Control 2010;4:23–5.
[67] Linderholm C, Jerndal E, Mattisson T, Lyngfelt A. Investigation of NiO-based mixed oxides in a 300-W chemical-looping combustor. Chem Eng Res Des 2010;88:661–72.
[68] Dueso C, García-Labiano F, Adánez J, de Diego LF, Gayán P, Abad A. Syngas combustion in a chemical-looping combustion system using an impregnated Ni-based oxygen carrier. Fuel 2009;88:2357–64.
[69] Adanez J, Abad A, Garcia-Labiano F, Gayan P, de Diego LF. Progress in chemical-looping combustion and reforming technologies. Prog Energy Combust Sci 2012;38:215–82.
[70] Otomo J, Oishi J, Mitsumori T, Iwasaki H, Yamada K. Evaluation of cost reduction potential for 1 kW class SOFC stack production: implications for SOFC technology scenario. Int J Hydrogen Energy 2013;38:14337–47.
[71] Kakaras E, Koumanakos AK, Doukelis A. Combined cycle systems for near-zero emission power generation. Woodhead Publishing; 2012.
[72] Fackrell JE. Aerodynamic effects on PFBC erosion target experiments. Wear 1989;134:237–52.
[73] Sasatsu H, Misawa N, Shimizu M, Abe R. Predicting the pressure drop across hot gas filter CTF installed in a commercial size PFBC system. Powder Technol 2001;118:58–67.
[74] Kunze C, De S, Spliethoff H. A novel IGCC plant with membrane oxygen separation and carbon capture by carbonation–calcinations loop. Int J Greenhouse Gas Control 2011;5:1176–83.